



REVIEW

Determination of mercury content in hard coal and fly ash using X-ray diffraction and scanning electron microscopy coupled with chemical analysis



Przemysław Rompalski^{a,*}, Adam Smoliński^b, Hanna Krztoń^c,
Jarosław Gazdowicz^c, Natalia Howaniec^b, Leokadia Róg^a

^a Department of Solid Fuels Quality Assessment, Central Mining Institute, Pl. Gwarków 1, 40-166 Katowice, Poland

^b Department of Energy Saving and Air Protection, Central Mining Institute, Pl. Gwarków 1, 40-166 Katowice, Poland

^c Department of Investigations of Properties and Structure of Materials, Instytut Metalurgii Żelaza, K. Miarki Str. 12-14, 44-100 Gliwice, Poland

Received 30 October 2015; accepted 26 February 2016

Available online 8 March 2016

KEYWORDS

Mercury;
Hard coal;
Fly ash;
XRD;
SEM/EDS

Abstract The objective of the work was testing the suitability of X-ray Diffraction (XRD) and Scanning Electron Microscopy with X-ray microanalysis (SEM/EDS-Energy Dispersive X-ray Spectroscopy) for qualitative assessment of mercury present in coals and furnace wastes (slag, ash). Such information is essential e.g. for determination of the potential effects of waste coal dumps on the environment (mercury compound emissions through leaching and erosion to water and soil). No minerals of mercury, i.e. containing mercury as a necessary and substantial component were identified with the application of the above mentioned techniques in studied hard coal and fly ash samples provided by a heat and power plant. In hard coal, mercury was detected as an impurity only in the alumina silicates. EDS spectra of pure coal grains did not show the emission lines of mercury. In fly ash, the minerals of mercury were also not detected; mercury was present in an amorphous component (mineral glass) and probably as an impurity in hauyne $\text{Na}_3\text{Ca}(\text{Si}_3\text{Al}_3)\text{O}_{12}(\text{SO}_4)$.

© 2016 The Authors. Published by Elsevier B.V. on behalf of King Saud University. This is an open access article under the CC BY-NC-ND license (<http://creativecommons.org/licenses/by-nc-nd/4.0/>).

* Corresponding author. Tel.: +48 32 2592609; fax: +48 32 2596533.

E-mail address: prompalski@gig.eu (P. Rompalski).

Peer review under responsibility of King Saud University.



Contents

1. Introduction	3928
2. Methods and materials	3929
3. Results and discussion	3934
4. Conclusions	3940
Acknowledgment.	3942
References	3942

1. Introduction

Coal is the major energy resource in Poland, providing approximately 90% of power production (Market Information Centre; Dubiński, 2013; Smoliński, 2008). The hard coal reserves in Poland amount to 19,485 Gt (Państwowy Instytut Geologiczny, 2015). It is also the essential energy source worldwide; the world coal consumption in energy sector (70% in 2010) is expected to increase by 1.3% per year according to the US Department of Energy forecast (International Energy Outlook, 2013). Mercury present in hard coal is released to the environment in the process of coal combustion. Most of mercury transfers into outlet gas, forming oxides, chlorides, nitrates, sulfates, and carbonates. Part of mercury is accumulated in furnace wastes, slags, and fly ash. Mercury cycle and chemical transformation of mercury during coal combustion have been previously described in the literature (Gostomczyk et al., 2010; Hławiczka et al., 2003; Smoliński, 2007; Yudovich and Ketris, 2005a, 2005b). Mercury is leached from coal wastes and landfills surface and migrates with water or it is transported to the air with ashes (Feng et al., 2002; Gibb et al., 2000; Glodek and Pacyna, 2009; Hower et al., 2005, 2010; Kłojzy-Karczmarczyk and Mazurek, 2010; Kostova et al., 2013; Niedzwiecki et al., 2007; Pacyna et al., 2010; Rubel et al., 2006; Sushil and Batra, 2006; Wang et al., 2010; Vejahati et al., 2010; Zhang et al., 2007). Qualitative recognition of mercury compounds in coals and furnace waste would, therefore, significantly contribute to the management of environmental aspects related to the effects of coal waste dumps on ground and water.

Mercury compounds have the strong impact on cell membranes of organisms, affecting various kinds of enzymatic reactions as well as the accumulation of mercury in human brain and kidneys. Therefore mercury is the third in the ranking of substance toxicity by the Agency for Toxic Substances and Disease Registry (ASDR) of 2013, just after arsenic and lead (Agency for Toxic Substances and Disease Registry (ATSDR) and Michalska, 2010).

The methods most commonly applied in studies of coal structure and properties include optical and electron microscopy; light absorption and reflection level; X-ray Diffraction, determination of density and colloid structure parameters; Visible, Ultraviolet and Infrared Spectroscopy (UV-VIS); Magnetic Resonance Spectroscopy (MRS); Electron Spin Resonance Spectroscopy (ESR); Nuclear Magnetic Resonance (NMR); and High Resolution Mass Spectrometry (HRMS).

Table 1 Proximate and ultimate analyses of the studied samples.

Parameter	Sample		
	PR1	PR2	PR3
Moisture, W (%w/w)	1.68 ± 0.30	1.58 ± 0.30	0.39 ± 0.10
Ash, A (%w/w)	23.18 ± 0.44	28.70 ± 0.30	93.70 ± 0.30
Carbon, C (%w/w)	61.57 ± 0.86	57.86 ± 0.42	5.93 ± 0.38
Sulfur, S (%w/w)	0.52 ± 0.04	1.00 ± 0.04	0.00 ± 0.01
Mercury, Hg (ppm)	0.09 ± 0.02	0.11 ± 0.02	0.42 ± 0.02

Table 2 Trace elements content in the ash obtained from studied samples.

Trace elements (ppm)	Sample		
	PR1	PR2	PR3
Ag	<2 ± 0.4	<2 ± 0.4	<2 ± 0.4
As	17 ± 3.4	17 ± 3.4	25 ± 5.0
Ba	611 ± 122.2	455 ± 91.0	620 ± 124.0
Cd	<2 ± 0.4	<2 ± 0.4	<2 ± 0.4
Co	52 ± 10.4	59 ± 11.8	108 ± 21.6
Cr	191 ± 38.2	200 ± 40.0	128 ± 25.6
Cu	95 ± 19.0	105 ± 21.0	158 ± 31.6
Mn	892 ± 178.4	796 ± 159.2	888 ± 177.6
Mo	<2 ± 0.4	<2 ± 0.4	<2 ± 0.4
Ni	147 ± 29.4	138 ± 27.6	101 ± 20.2
Pb	87 ± 17.4	74 ± 14.8	331 ± 66.2
Rb	156 ± 31.2	152 ± 30.4	158 ± 31.6
Sb	<2 ± 0.4	<2 ± 0.4	4 ± 0.8
Sn	3 ± 0.6	7 ± 1.4	8 ± 1.6
Sr	464 ± 92.8	365 ± 73.0	461 ± 92.2
V	187 ± 37.4	179 ± 35.8	183 ± 36.6
Zn	230 ± 46.0	258 ± 51.6	1305 ± 261.0

Table 3 Oxides content in the ash obtained from studied samples.

Oxides (%w/w)	Sample		
	PR1	PR2	PR3
SiO ₂	51.43 ± 3.09	52.93 ± 3.18	55.37 ± 3.32
Al ₂ O ₃	25.70 ± 3.08	25.91 ± 3.11	24.30 ± 2.92
Fe ₂ O ₃	7.51 ± 0.60	8.50 ± 0.68	6.89 ± 0.55
CaO	3.50 ± 0.28	2.52 ± 0.20	3.91 ± 0.31
MgO	3.01 ± 0.54	2.30 ± 0.41	2.53 ± 0.46
Na ₂ O	1.31 ± 0.31	0.61 ± 0.15	0.98 ± 0.24
K ₂ O	3.03 ± 0.30	2.75 ± 0.28	3.39 ± 0.34
SO ₃	2.33 ± 0.42	2.51 ± 0.45	0.44 ± 0.08
TiO ₂	1.04 ± 0.12	1.01 ± 0.12	1.03 ± 0.12
P ₂ O ₅	0.26 ± 0.04	0.18 ± 0.03	0.34 ± 0.05

Physical methods enable testing of coal in unchanged form and determination of such specific parameters as surface chemical state and functional groups. The drawback of these methods is lack of standard substances enabling objective and unambiguous interpretation of the results (Jasieńska, 1995).

In this work, X-ray Diffraction (XRD) and Scanning Electron Microscopy with X-ray microanalysis (SEM/EDS) were selected to study the chemical and mineral composition of coal and fly ash.

The most common application of the XRD method is an identification of a crystalline chemical compound (or compounds) in a polycrystalline material (Dinnebier and Billinge, 2008; Klug and Alexander,

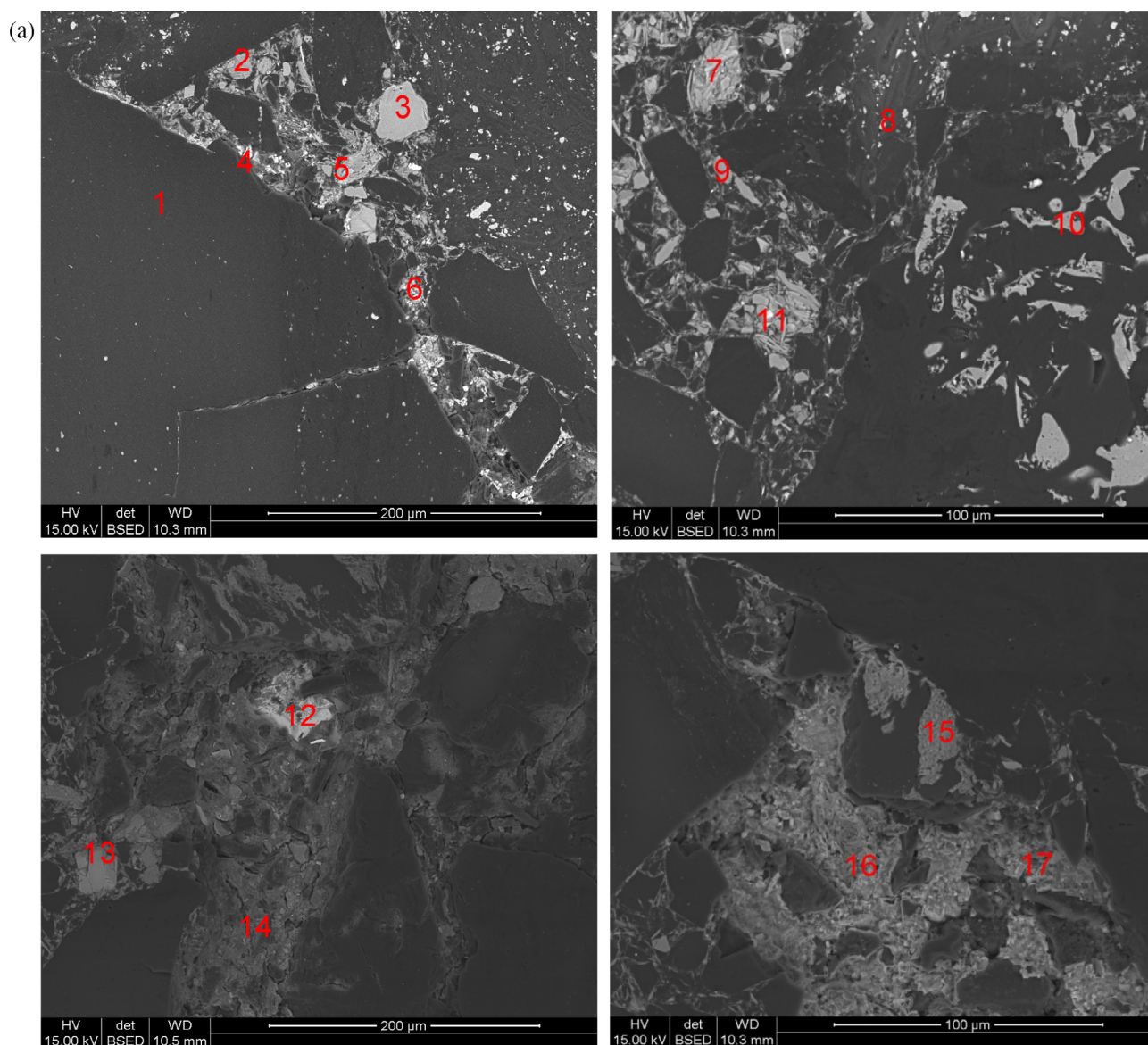


Figure 1 (a) The backscattered electron micrographs of the polished section of the PR1 sample of hard coal and (b) the corresponding results of chemical analysis in the micro areas indicated by numbers 1–6.

1974). Each crystalline chemical compound (including minerals) is characterized by its own experimental diffraction pattern with two important distinguishing features: the positions of the diffraction lines and their intensities in the diffraction pattern. This characteristic diffraction pattern reflects the crystalline structure of the phase, which allows to distinguishing among various polymorphs of the same chemical compound (e.g. SiO_2 , which can form six different crystalline polymorphs and one amorphous phase).

The experimental diffraction pattern of a phase can vary from the standard diffraction data. This is due to the presence of foreign atoms, forming the solid solution in the crystalline net. These atoms do not form their own compounds, so their presence in the minerals can be detected only by some chemical methods; in this study scanning electron microscopy (SEM) with EDS detector was applied to analyze the chemical composition in micro regions. The Rietveld method (Rietveld, 1967, 1969) was used to quantify the mineral constituents of the samples.

The aim of this study was the determination of the level of mercury content and its form of occurrence (mercury minerals or mercury built-in in the crystalline net of other minerals) in coals and furnace wastes.

The determination of chemical and mineral composition of coal and fly ash, with the application of X-ray Diffraction (XRD) and Scanning Electron Microscopy with X-ray microanalysis (SEM/EDS) methods was performed.

2. Methods and materials

Two samples of hard coal (PR1 and PR2) and one sample of ash (PR3), resulting from the combustion of PR1 coal were collected in a power plant located in the Silesia region, Poland, according to the standards PN-G-04502: 1990 (applicable to hard coal) and BN-81-0623-01 (for slag, ash, and slag-ash mixtures).

The physical and chemical parameters of hard coals and fly ash in analytical state were analyzed in Department of Solid Fuels Quality Assessment of the Central Mining Institute. Moisture and ash contents were determined based on PN-G-04560: 1998 and PN-ISO 1171:2002 standards with the appli-

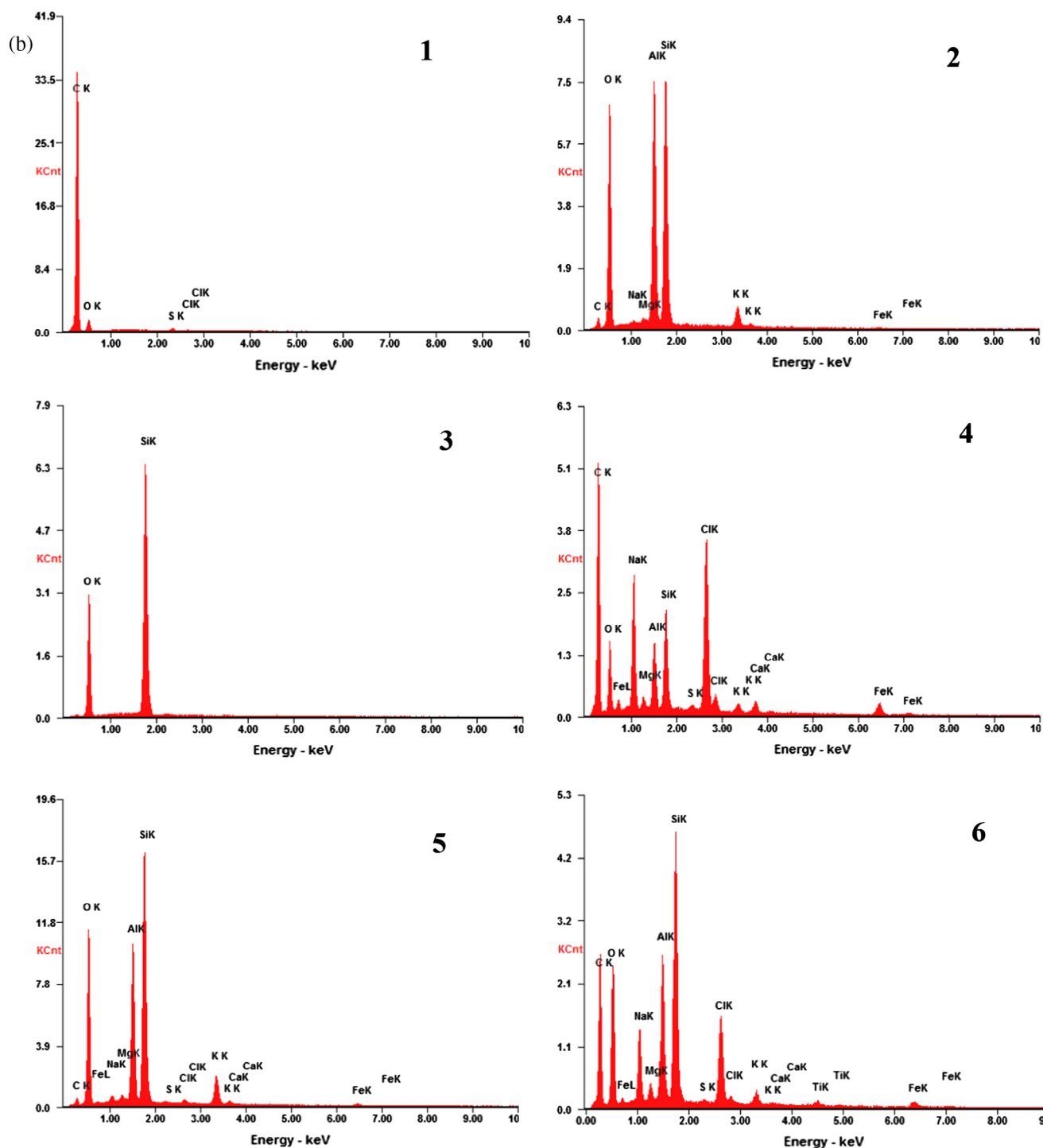


Fig. 1 (continued)

cation of LECO thermogravimetric analyzer. Carbon and sulfur contents were determined with the use of high-temperature combustion with infrared detector technique using ITR ACS-40/1500 (Tele- and Radio Research Institute) and 628CHNS LECO analyzers, respectively. The latter analyses were performed in accordance with standards PN-G-04571:1998 and PN-G-04584:2001, respectively. Mercury content was determined in the Department of Environmental Monitoring of

the Central Mining Institute with the application of high-temperature combustion coupled with Cold Vapor Atomic Absorption Spectrometry (CVAAS) and the gold amalgamation process, using MA-2000 Nippon Instrument Corporation. The results are given in Table 1.

Ash samples were also prepared from the PR1-PR3 materials and analyzed in terms of trace elements and oxide contents in the Department of Environmental Monitoring of the Cen-

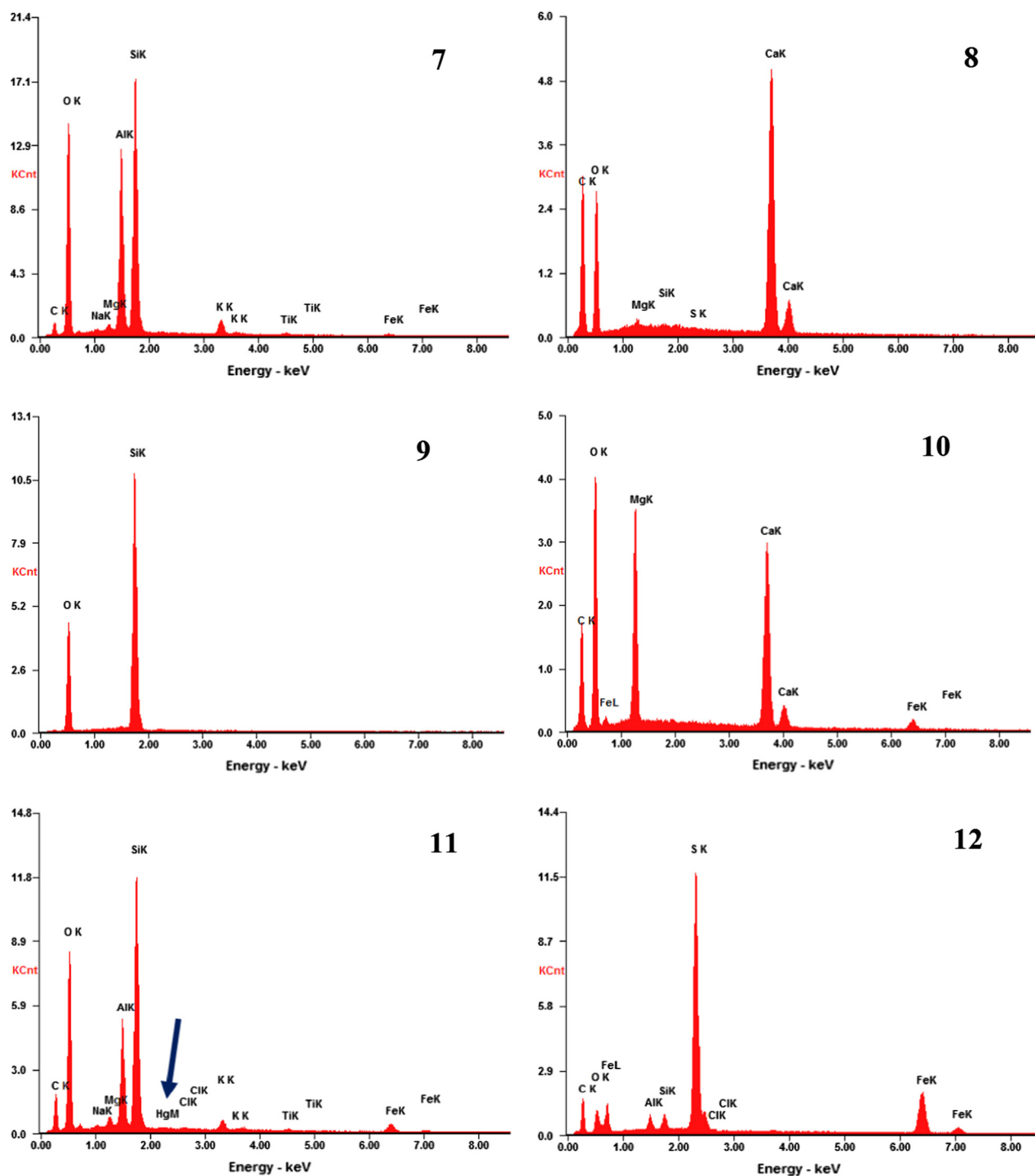


Fig. 1 (continued)

tral Mining Institute with the application of X-ray Fluorescence technique and ZSX Pymus II, RIGAKU instrument (see Tables 2 and 3). The pellets were made by pressing the ash with graphite.

Two fractions, mineral and organic, were obtained in the dense liquid (1.4 g/cm^3) separation process of the samples tested. The analysis of each fraction enabled more in-depth assessment of the presence of mercury compounds in the samples tested.

The samples for XRD experiments were ground in a Fritsch Pulverisette 0 mill. The XRD diffraction patterns were obtained using filtered Fe $K\alpha$ radiation and a PANalytical Empyrean diffractometer equipped with a high efficient, solid-state PIXcel detector. The identification of minerals was performed with the application of standard diffraction data of Powder Diffraction File PDF-4+, updated and released yearly by the International Centre for Diffraction Data, USA. There is no limit concerned with the number of

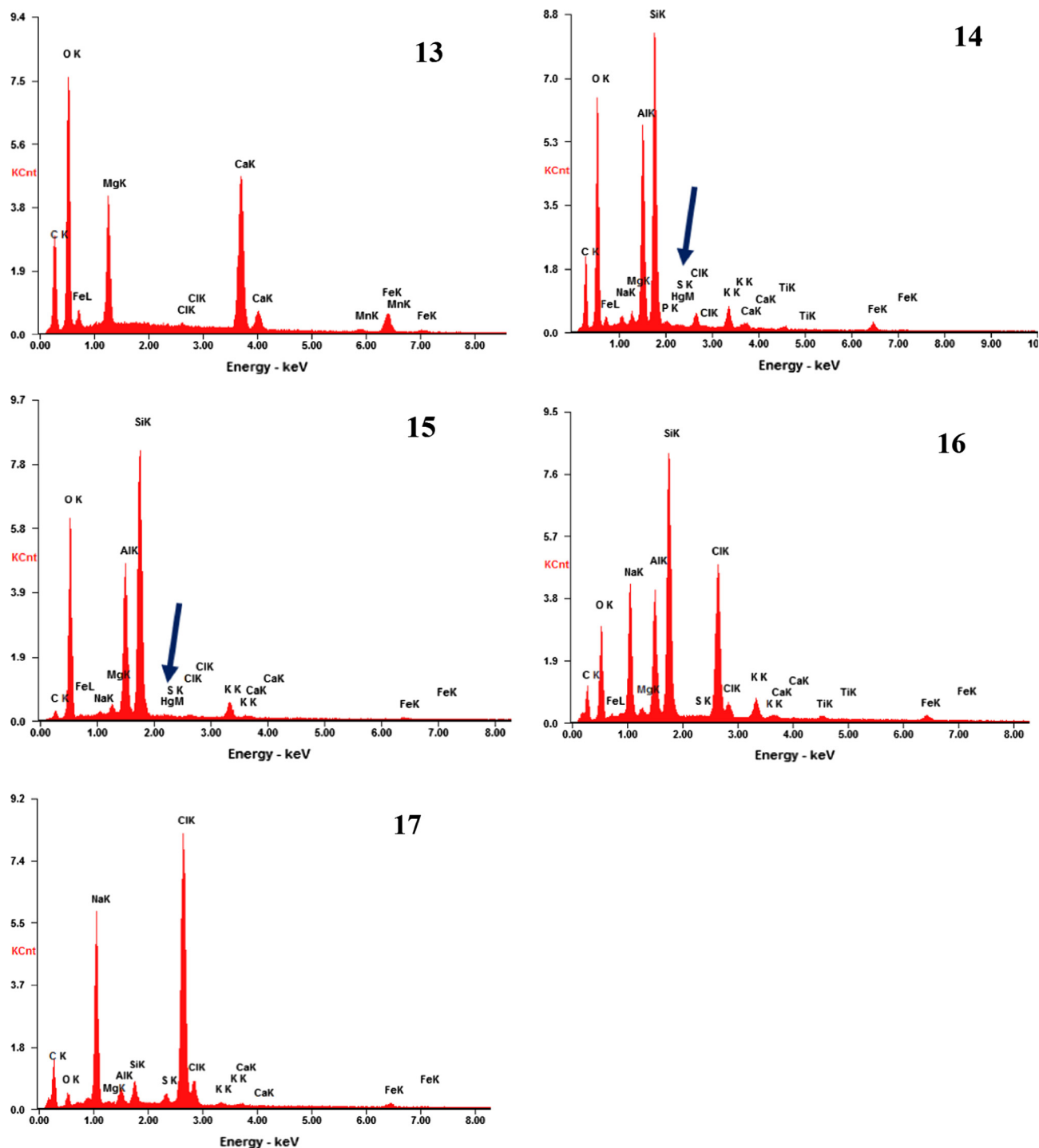


Fig. 1 (continued)

possible identified phases but a detection limit of a mineral in the XRD studies depends on its structure and the coexisting minerals, forming the matrix. The published XRD detection limits for various minerals (Ferret, 2000) showed significant differences depending on the iron content in a sample. The detection limit of quartz changed from 0.12 wt% to 0.5 wt%; for kaolinite – from 1.7 wt% to 7.8 wt%, for the lower and the higher content of iron, respectively. In such a light matrix as coal and also as fly ash, the detection limits of many minerals

are usually very low – much below 1.0 wt%. The quantitative phase analysis was done using the Rietveld method and the SIROQUANT™ software. The software can be used to analyze and quantify up to 25 crystalline phases simultaneously and, in the same time, an additional constituent – the amorphous phase. The structural data of mineral constituents of the examined samples were taken from the PDF-4+ base. Powdered corundum, the certified Standard Reference Material No. 676a, produced by National Institute for Standards and Tech-

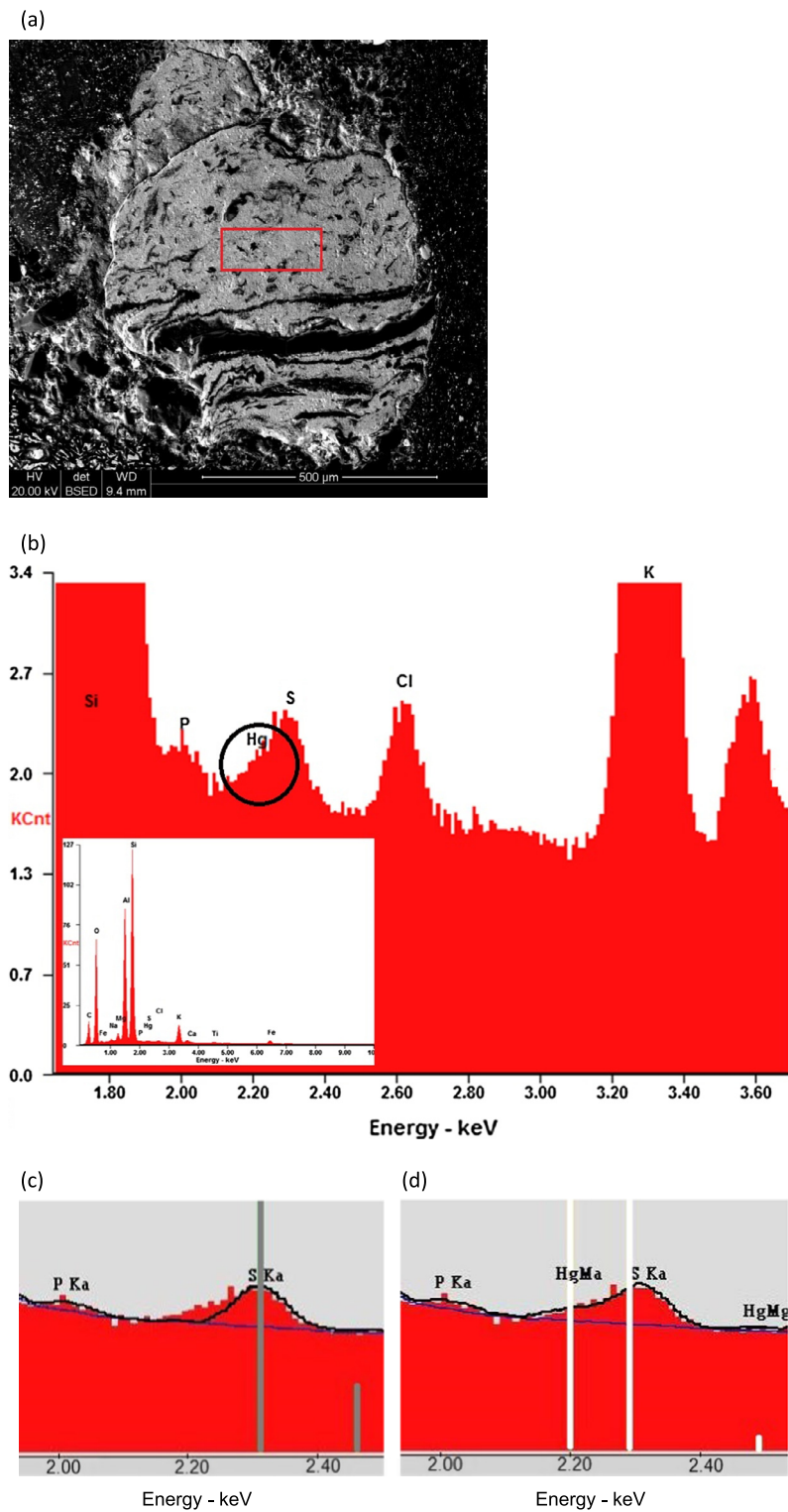


Figure 2 The polished section of the PR1 sample of hard coal. (a) The backscattered electron micrograph of a mineral grain, (b) the details of the collected spectrum from the area marked in (a) and the entire spectrum (the emission line of Hg is marked with a circle), the parts of energy spectrum with the fitted emission standard lines of sulfur (gray lines) and phosphor (c), and phosphor, sulfur and mercury (white lines) (d).

nology (USA), was used as a spike phase to detect and quantify the organic part (the hard coal samples) and the amorphous component (the fly ash sample).

The morphology of powder particles was analyzed with the application of Inspect F scanning electron microscope. The chemical analysis of microareas was performed with the appli-

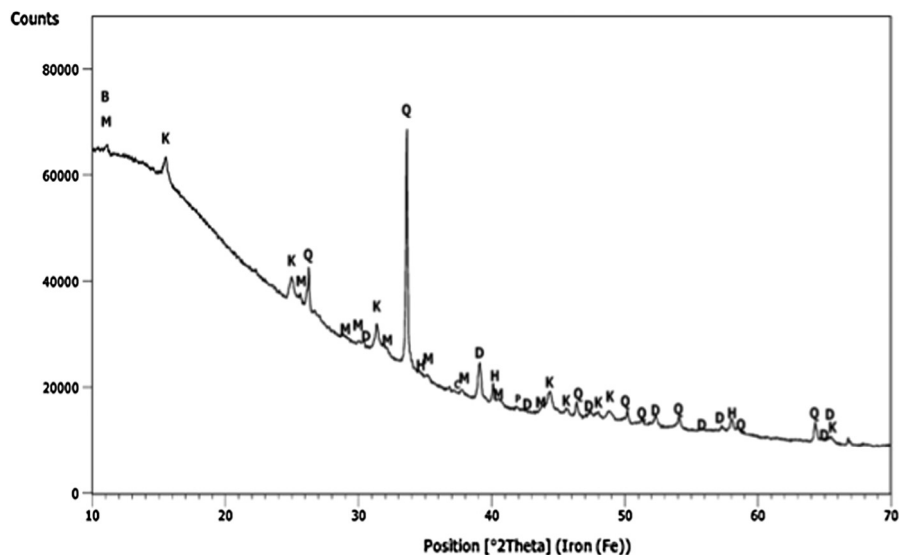


Figure 3 The experimental diffraction pattern of the PR1 sample of hard coal. The most intense diffraction lines of the individual phases are indicated with letters Q – quartz, K – kaolinite, M – muscovite, B – biotite, P – pyrite, D – dolomite, and H – halite.

cation of EDS detector. The particles of the PR3 sample (fly ash) were glued to a sample holder using carbon glue to remove the built-up electric charge from the holder. The PR1 and PR2 samples (hard coal) were prepared as the metallographic specimens. Both kinds of studies (XRD and SEM-EDS) were carried out in the Instytut Metalurgii Żelaza.

3. Results and discussion

The mineral composition of the PR1 sample was determined based on the analysis of the mineral fraction resulting from the dense liquid separation of the sample. The SEM-EDS data are presented in Fig. 1, showing the SEM/BSE images and the

spectra of various minerals, forming the mineral matter of coal. The letters M and K in Figs. 1, 4 and 7 represent the characteristic X-ray emission lines of mercury and the remaining elements, respectively. Spectrum 3 and 9 correspond to quartz, and spectra 8, 10, and 13 refer to carbonates: calcite and dolomite. The presence of halite is proved by spectra 4, 6, 16, and 17, and the content of pyrite is indicated by spectrum 12. There are six spectra of alumina silicates (denoted 2, 5, 7, 11, 14, and 15); three of them contain traces of mercury. Arrows in Fig. 1 indicate the position of a characteristic X-ray M line of mercury. Furthermore, very weak lines of mercury can be found on emission spectra of alumina silicates, contain-

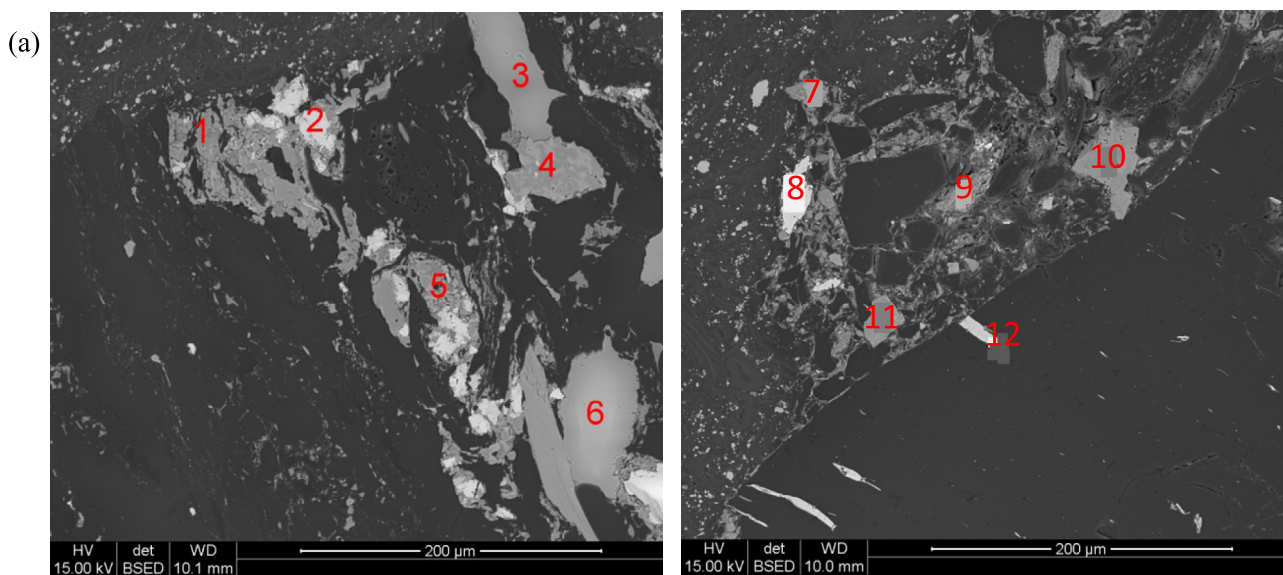


Figure 4 (a) The backscattered electron micrographs of the polished section of the PR2 sample of hard coal and (b) the corresponding results of chemical analysis in the micro areas indicated by numbers 1–12.

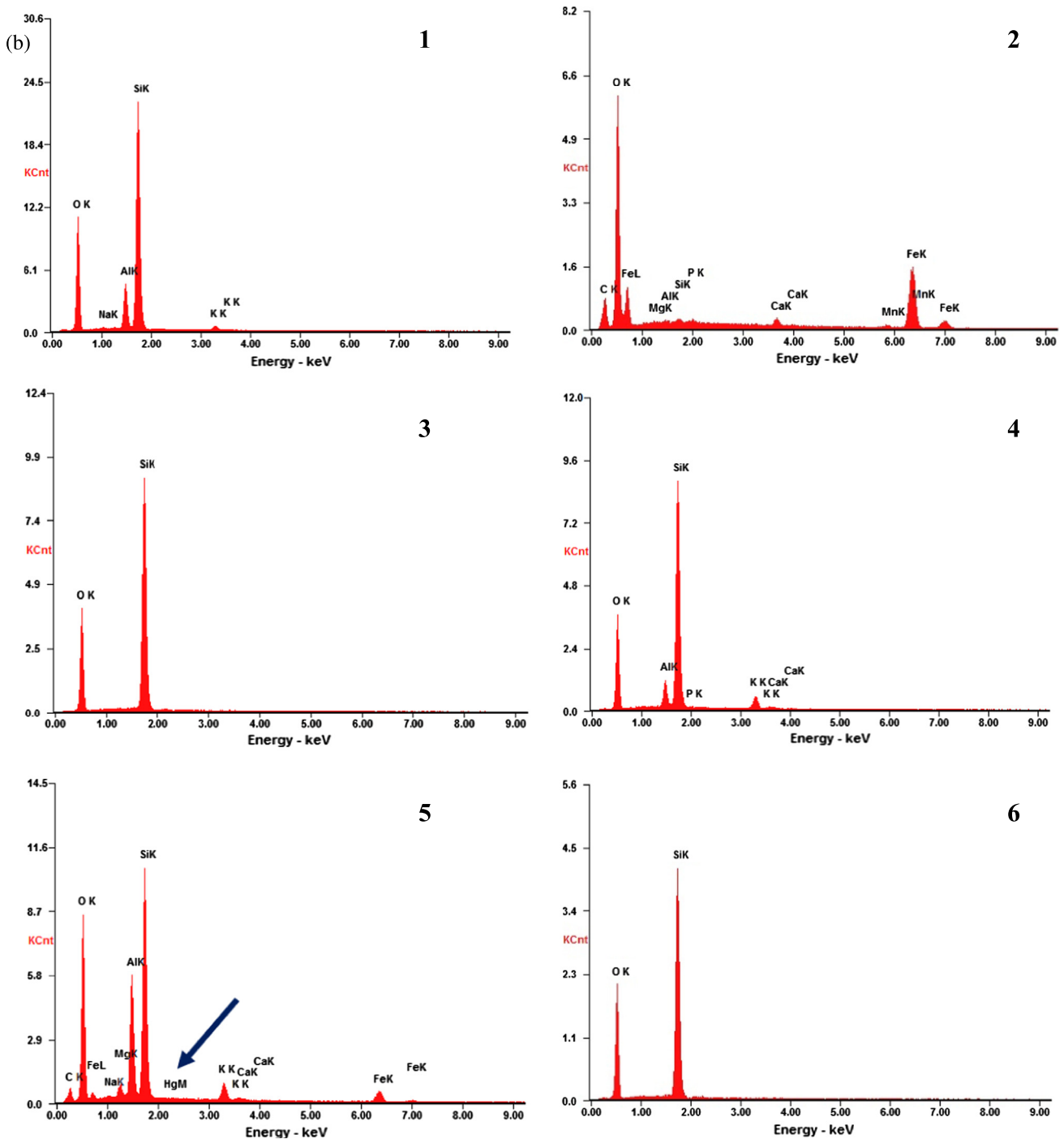


Fig. 4 (continued)

ing also potassium, sodium, magnesium, iron, titanium, calcium, chlorine, and sulfur (spectra 11, 14, and 15). It can be clearly seen that in the PR1 sample of hard coal only one type of minerals grains contains traces of mercury, i.e. some grains of alumina silicates. The analyzed grains of coal showed no traces of mercury (spectrum 1).

Fig. 2 shows the backscattered electron micrograph of a selected mineral grain of the PR1 sample containing mainly aluminum, silicon and oxygen (Fig. 2a), the details of the col-

lected spectrum from the marked area of the PR1 sample and the entire spectrum (Fig. 2b). Below, the part of the spectra is shown with the fit of the standard emission lines of phosphorus and sulfur to the experimental data (Fig. 2c). The line of low intensity of mercury, partly overlapping with the line of sulfur, is clearly seen. The final fit of the phosphorus, sulfur and mercury lines is presented in Fig. 2d.

The diffraction pattern of the PR1 sample of hard coal is presented in Fig. 3. Because of the considerable total number

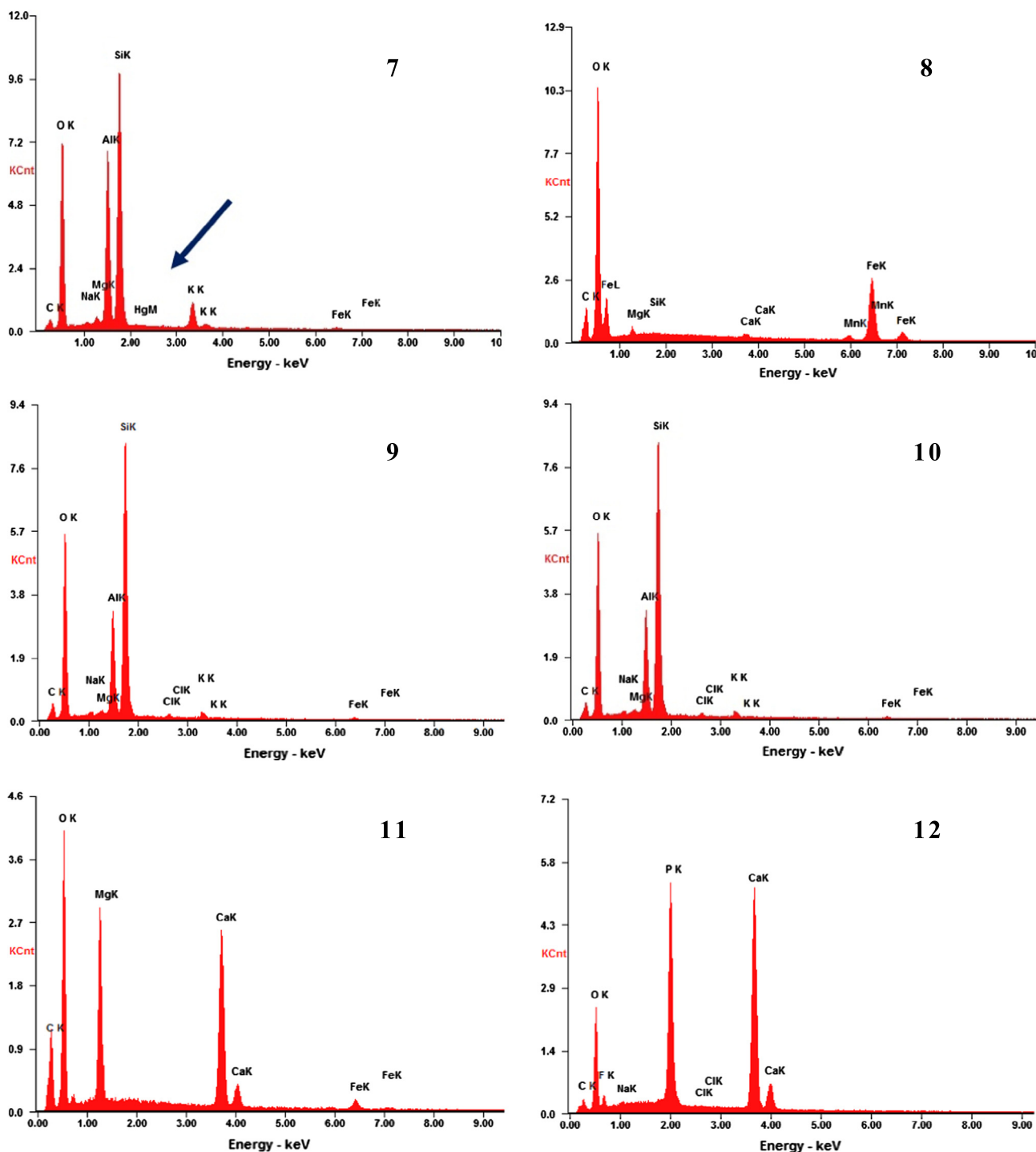


Fig. 4 (continued)

of the diffraction lines (reflexes) of the identified minerals in the presented range of the diffraction pattern, only the strongest diffraction lines of the mineral constituents of the sample are marked by letters.

The results of a quantitative phase analysis of the mineral matter of coal (see Table 4) show that it was formed mainly by quartz, kaolinite, muscovite, and illite. Carbonates, such as dolomite and traces of calcite, were also present. The frac-

tions of pyrite and halite were below 0.5%w/w. The values of errors shown in Table 4 (and in Tables 5 and 6) contain both statistical and systematic components (Taylor and Hinczak, 2001).

No crystalline mercury compounds were identified in the phase analysis process. The parallel examination of the SEM-EDS and the XRD results showed that mercury was present as an impurity in some alumina silicates.

Table 4 The results of minerals identification and quantitative phase analysis of inorganic matter of the PR1 sample. The residue is the non-crystalline organic matter – coal and other possible amorphous minerals. The values of the errors contain both statistical and systematical components. The space group symbols of the individual crystalline phases are included.

Mineral	Space group	Fraction (%w/w)
Quartz, SiO ₂	<i>P3₂21</i>	4.0 ± 0.8
Kaolinite, Al ₂ Si ₂ O ₅ (OH) ₄	<i>C1</i>	3.8 ± 0.8
Muscovite, KAl ₂ Si ₄ O ₁₀ (OH) ₂	<i>C2/c</i>	4.4 ± 1.6
Illite, (K, H ₃ O)Al ₂ Si ₃ AlO ₁₀ (OH) ₂	<i>C2/c</i>	2.6 ± 1.6
Biotite, KFeMg ₂ (AlSi ₃ O ₁₀)(OH) ₂	<i>C2/m</i>	< 0.5 ± 0.1
Dolomite, CaMg(CO ₃) ₂	<i>R-3</i>	2.4 ± 0.8
Calcite, CaCO ₃	<i>R-3c</i>	< 0.5 ± 0.1
Pyrite, FeS ₂	<i>Pa-3</i>	< 0.5 ± 0.1
Halite, NaCl	<i>Fm-3m</i>	< 0.5 ± 0.1
Gypsum, CaSO ₄ ·2H ₂ O	<i>C2/c</i>	< 0.5 ± 0.1
Total amount of crystalline mineral matter		18.4
The residue – coal and possible amorphous minerals		81.6 ± 2.4

Table 5 The results of minerals identification and quantitative phase analysis of inorganic matter of the PR2 sample. The residue is the non-crystalline organic matter – coal and other possible amorphous minerals. The values of the errors contain both statistical and systematical components. The space group symbols of the individual crystalline phases are included.

Mineral	Space group	Fraction (%w/w)
Quartz, SiO ₂	<i>P3₂21</i>	5.8 ± 1.0
Kaolinite, Al ₂ Si ₂ O ₅ (OH) ₄	<i>C1</i>	5.0 ± 1.0
Chamosite, (Fe, Al, Mg) ₆ (Si, Al) ₄ O ₁₀ (OH) ₈	<i>C2/m</i>	< 0.5 ± 0.1
Muscovite, KAl ₂ Si ₄ O ₁₀ (OH) ₂	<i>C2/c</i>	4.4 ± 2.0
Illite, (K, H ₃ O)Al ₂ Si ₃ AlO ₁₀ (OH) ₂	<i>C2/c</i>	2.0 ± 1.0
Biotite, KFeMg ₂ (AlSi ₃ O ₁₀)(OH) ₂	<i>C2/m</i>	1.4 ± 1.0
Dolomite, CaMg(CO ₃) ₂	<i>R-3</i>	< 0.5 ± 0.1
Calcite, CaCO ₃	<i>R-3c</i>	0.5 ± 0.1
Siderite, FeCO ₃	<i>R-3c</i>	0.5 ± 0.1
Pyrite, FeS ₂	<i>Pa-3</i>	< 0.5 ± 0.1
Halite, NaCl	<i>Fm-3m</i>	< 0.5 ± 0.1
Magnetite, Fe ₃ O ₄	<i>Fd-3m</i>	< 0.5 ± 0.1
Hematite, Fe ₂ O ₃	<i>R-3c</i>	< 0.5 ± 0.1
Goethite, α-FeO(OH)	<i>Pbnm</i>	< 0.5 ± 0.1
Rutile, TiO ₂	<i>PA₂/mmm</i>	< 0.5 ± 0.1
Total amount of crystalline mineral matter		20.6
The residue – coal and possible amorphous minerals		79.4 ± 4.2

The results of SEM/EDS analysis of mineral fraction and characteristic of the PR2 sample are given in Fig. 4. As in the case of the PR1 sample, as many as possible results of the local chemical analysis of the minerals grains are shown to present the variety of the existing minerals. Spectrum 2 (light grains in Fig. 4a) corresponds to iron oxides; spectra 3 and 6 (light gray grains in Fig. 4a) relate to quartz; spectra

Table 6 The results of minerals identification and quantitative phase analysis of inorganic matter of the PR3 sample. The residue is the amorphous phase. The values of the errors contain both statistical and systematical components. The space group symbols of the individual crystalline phases are included.

Mineral	Space group	Fraction (%w/w)
Quartz, SiO ₂	<i>P3₂21</i>	10.0 ± 0.4
Mullite, Al ₆ Si ₂ O ₁₃	<i>Pbam</i>	11.1 ± 0.4
Lime, CaO	<i>Fm-3m</i>	< 0.5 ± 0.1
Calcite, CaCO ₃	<i>R-3c</i>	< 0.5 ± 0.1
Anhydrite, CaSO ₄	<i>Bmmb</i>	< 0.5 ± 0.1
Periclase, MgO	<i>Fm-3m</i>	0.9 ± 0.4
Magnetite, Fe ₃ O ₄	<i>Fd-3m</i>	0.7 ± 0.4
Hematite, α-Fe ₂ O ₃	<i>R-3c</i>	< 0.5 ± 0.1
Rutile, TiO ₂	<i>P4₂/mmm</i>	< 0.5 ± 0.1
Hauyne, Na ₃ Ca(Si ₃ Al ₃)O ₁₂ (SO ₄)	<i>P-43n</i>	< 0.5 ± 0.1
The residue – amorphous component (mineral glass)		75.9 ± 1.8

1, 4, 5, 7, 9, and 10 indicate two kinds of alumina silicates. Carbonates containing calcium and magnesium (probably dolomite) are presented on spectrum 11 (Fig. 4b). Arrows indicate the position of a small characteristic X-ray M line of mercury in the spectrum of alumina silicate (see spectra 5 and 7 in Fig. 4b). Similarly like in the PR1 sample, mercury was observed only in the grains containing mainly aluminum, silicon and oxygen.

The identified three main crystalline components of the inorganic matter of the PR2 sample were quartz, kaolinite, and muscovite (see Table 5 and Fig. 5). The total number of diffraction lines was also significantly high (over two hundred). The positions of the strongest ones are marked by letters in Fig. 5. Illite, biotite, and chamosite were also detected, but at over twofold lower contents. The fraction of carbonates was the largest among the remaining group of minerals covering also oxides, sulfides, and chlorides. The oxides group was represented mainly by iron oxides (magnetite, hematite, and goethite). A small amount of rutile was also detected.

The observed diffraction lines did not fit any minerals of mercury (see Fig. 5). Based on the analysis of the diffraction data and the results of chemical analysis in micro areas (Figs. 4 and 6) it may be deduced that the atoms of mercury can be found as impurities forming solid solutions in alumina silicates containing iron. There are at least two minerals containing iron: chamosite and biotite. No traces of mercury were observed in the grains of coal.

In Fig. 6 the backscattered electron micrograph of a mineral grain, containing mercury, the details of the collected spectrum from the marked area of the PR2 sample and the entire spectrum are shown. The emission line of small intensity of mercury is observed in the vicinity of the line of sulfur.

The results of SEM/EDS analysis of the ash sample (PR3) are shown in Fig. 7. The large gray grains, consist of aluminum, silicon and oxide (as the major elements – spectra 1, 2, 4, 5, and 7–9) and also of potassium, magnesium, sodium, calcium, iron, sulfur and, in some grains, mercury (spectra 1, 8, 9), whereas the light gray grains correspond to iron oxides – the spectra Nos. 3, 6, and 10. The black area in Fig. 7a rep-

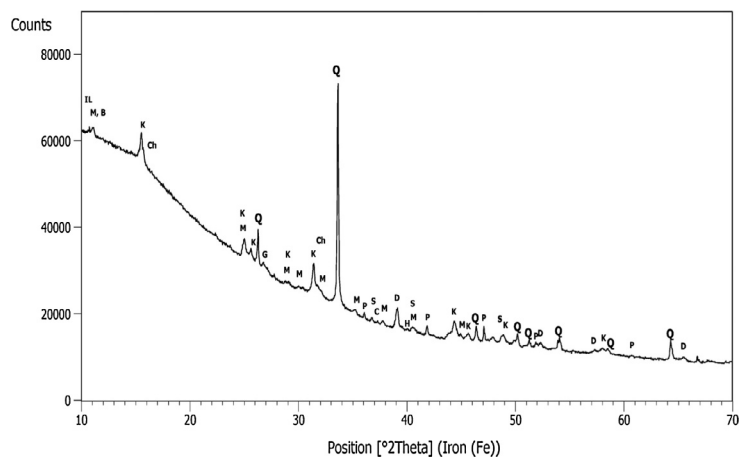


Figure 5 The experimental diffraction pattern of the PR2 sample of hard coal. The diffraction lines of the individual phases are indicated with letters Q – quartz, K – kaolinite, M – muscovite, B – biotite, IL –illite, Ch – chamosite, G – goethite, P – pyrite, D – dolomite, S – siderite, and H – halite.

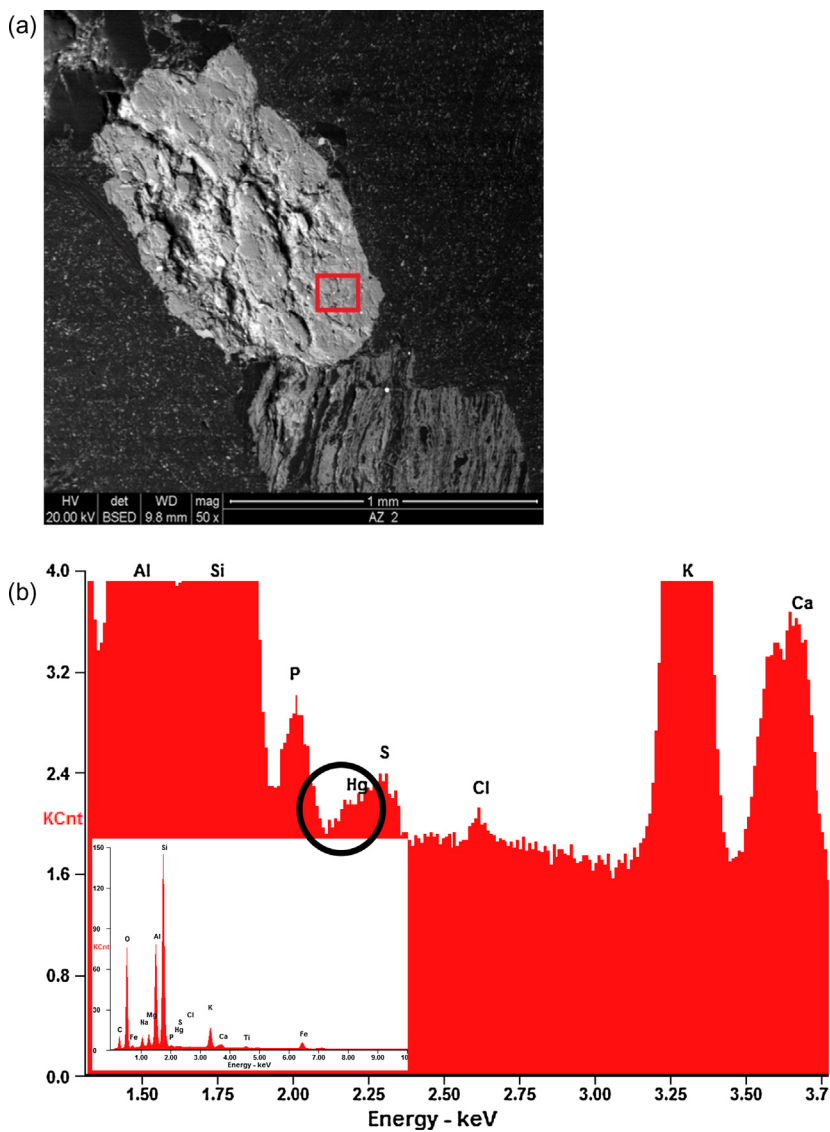


Figure 6 The polished section *n* of the PR2 sample of hard coal. (a) The backscattered electron micrograph of a mineral grain and (b) the details of the collected spectrum from the area marked in (a) and the entire spectrum (the emission line of Hg is marked with a circle).

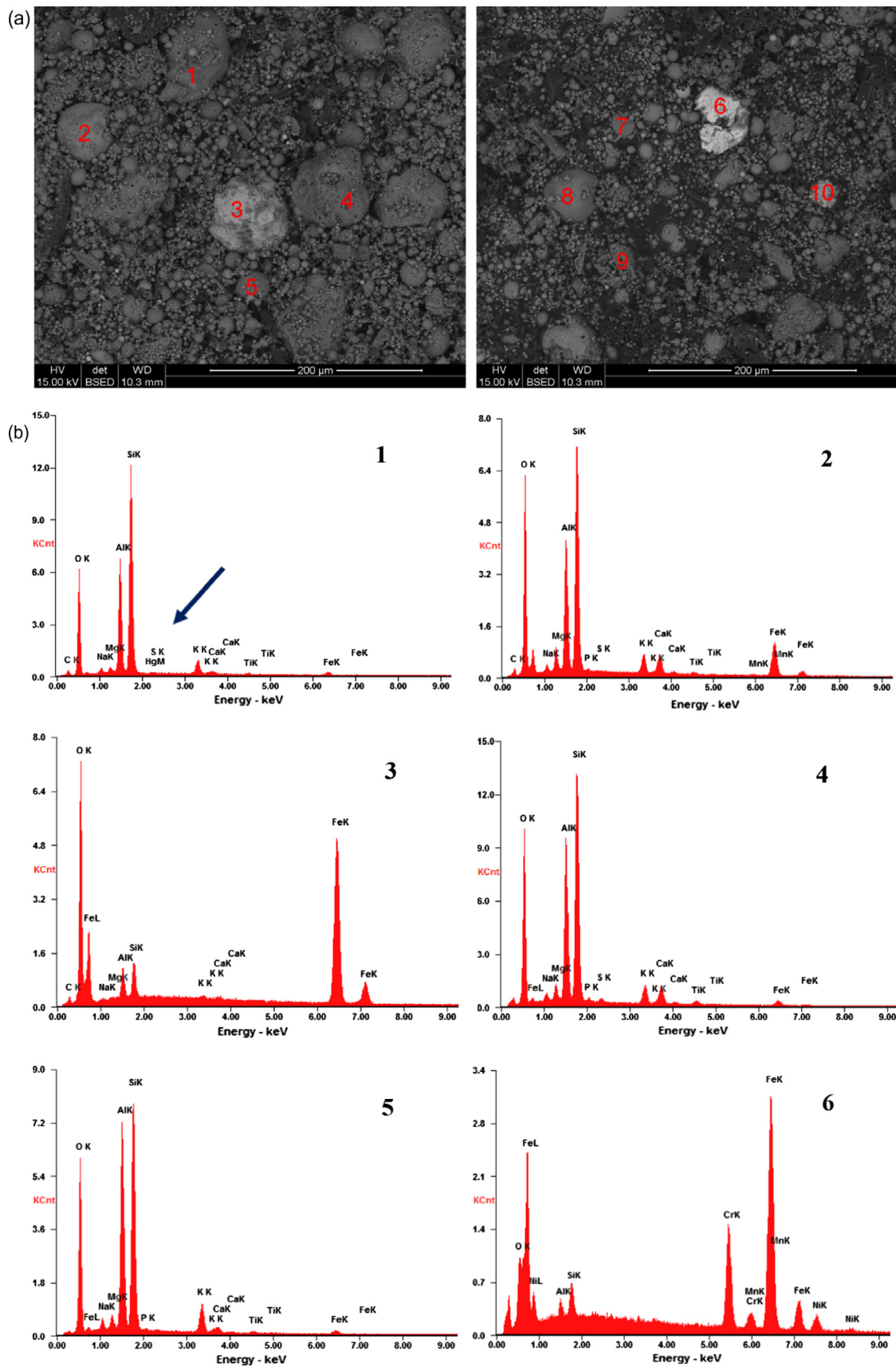


Figure 7 The particles of the PR3 sample (fly ash) glued to a sample holder using carbon glue. (a) The backscattered electron micrographs of the particles of the sample PR3 and (b) the corresponding results of chemical analysis in the micro areas indicated by numbers 1–10.

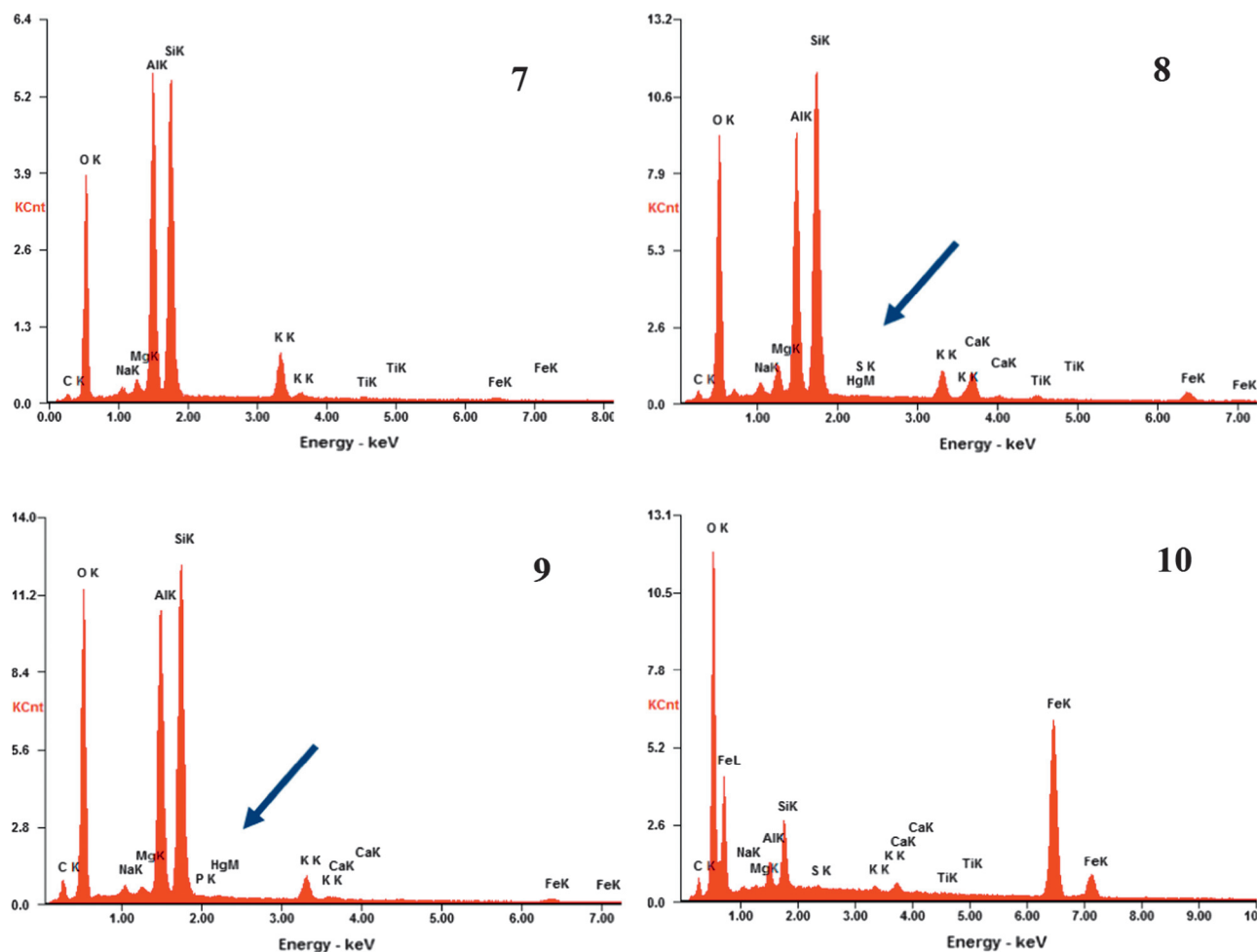


Fig. 7 (continued)

resents resin. Arrows in the spectra indicate the position of a characteristic X-ray M line of mercury.

Fig. 8 depicts the backscattered electron micrograph of a mineral grain (Fig. 8a), the details of the collected spectrum from the marked area of the PR3 sample with the entire spectrum (Fig. 8b) and the fit of the standard emission lines of mercury to the experimental spectrum (Fig. 8c). The fit of the phosphorus emission lines is also included.

The diffraction pattern of the PR3 sample is presented in Fig. 9; the insert in Fig. 9 shows the part of the diffraction pattern with the markers corresponding to the positions of the diffraction lines of individual minerals. The position of the strongest diffraction line of hauyne is marked in black. The results of quantitative phase analysis of the mineral matter are given in Table 6. The mineral glass (amorphous component) was the dominant constituent of the sample. The crystalline part of the sample consisted of several minerals, with the highest fractions of quartz, and mullite. Magnetite and periclase contents were approximately 1%w/w, and the concentrations of the remaining minerals were below 0.5%w/w. The minerals of mercury were not detected in the examined sample.

The results of the chemical analysis in micro areas proved that mercury was present in mineral particles containing aluminum, silica, oxygen, magnesium, calcium, potassium, and

sodium. Such chemical composition (excluded mercury) is typical of amorphous particles in fly ash (Kutchko and Kim, 2006). Some additions of iron and titanium were also observed in these kind of particles in the PR3 sample. The presence of sulfur (spectra no. 1, 8 in Fig. 7) and hauyne (diffraction pattern in Fig. 9) implies that mercury was also included as an impurity in hauyne.

4. Conclusions

The techniques applied proved to be useful for detection of the mercury presence and the identification of the form of its occurrence in coals and furnace wastes. The analysis of the EDS spectra enabled identification of the particular elements in the examined areas of coal and ash samples. These also allowed the accurate, qualitative estimation of mercury occurrence in the furnace waste. The Rietveld quantitative phase analysis provided the information on the quantities of minerals containing additions of mercury in coal and fly ash samples.

With this information, it is possible to predict the impact of combustion waste landfill on the environment, in particular the emissions of mercury compounds through leaching and erosion to water and soil. The results of XRD and SEM/EDS studies indicated that minerals of mercury were not present

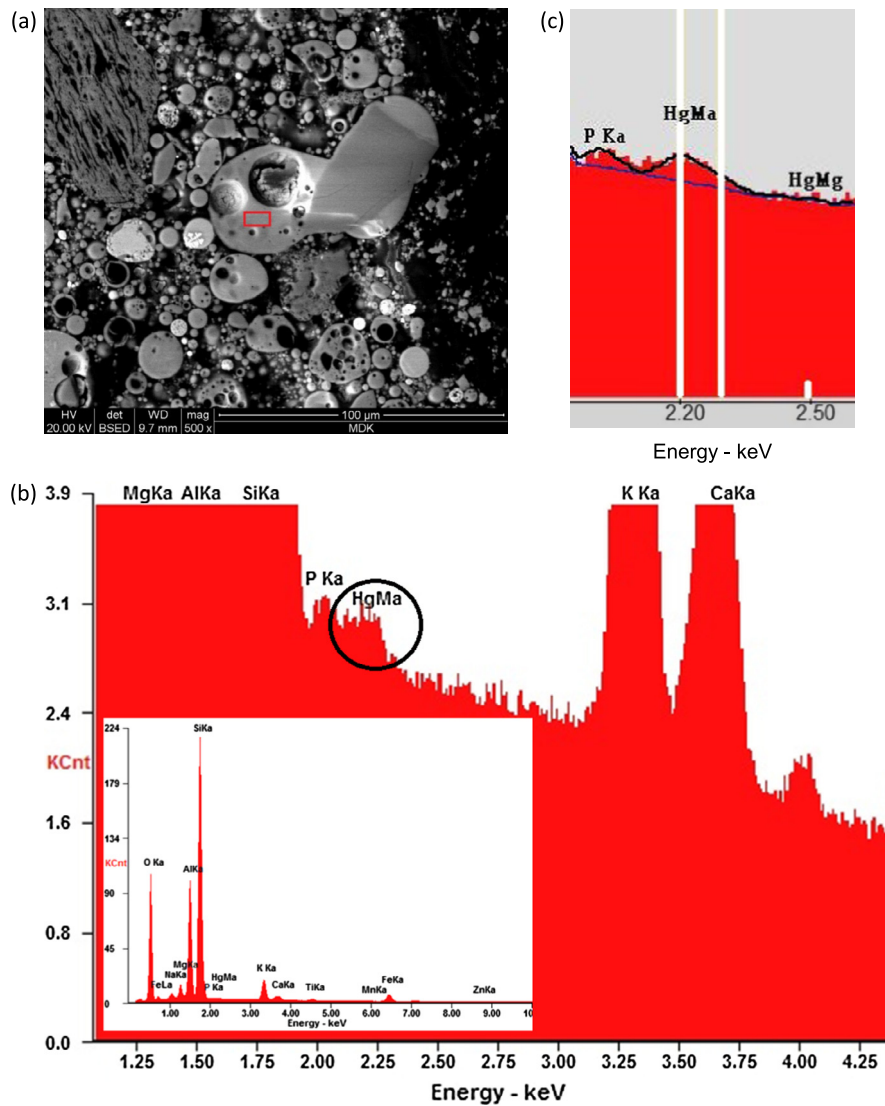


Figure 8 The polished section of the PR3 sample of fly ash. (a) The backscattered electron micrographs of mineral grains and (b) the details of the collected spectrum from the area marked in (a) and the entire spectrum. The emission line of Hg is marked with a circle. In Fig. 8(c), the fit of the emission lines of phosphorus and mercury is shown. The white lines represent the mercury emission lines.

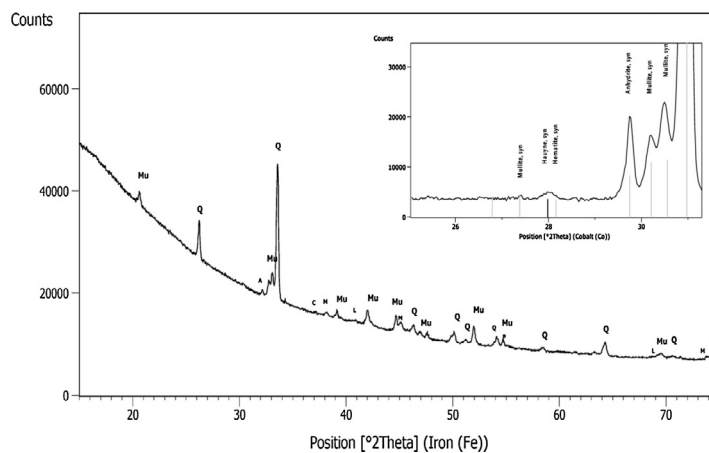


Figure 9 The experimental diffraction pattern of the PR3 sample of fly ash. The diffraction lines of the individual phases are indicated with letters Q – quartz, Mu – mullite, C – calcite, L – lime, P – periclase, M – magnetite, and A – anhydrite. The insert in the upper right corner shows the part of the diffraction pattern containing the most intense lines of haunyne (black marker), and anhydrite, mullite and quartz (gray markers). The strongest quartz line is the first on the right.

in the studied samples. In both coal samples mercury was detected as an impurity in alumina silicates grains; in the second coal sample mercury was found in alumina silicates containing iron. The EDS spectra of pure coal grains did not show any emission lines of mercury. In the fly ash sample, mercury was identified in an amorphous component (mineral glass) and, probably, in hauyne.

Acknowledgment

The research was conducted under the Project # 11320333-380, financed by the Ministry of Science and Higher Education, Poland.

References

- Agency for Toxic Substances and Disease Registry (ATSDR). Priority List of Hazardous Substances. <<http://www.atsdr.cdc.gov/SPL/index.html>> .
- Dinnebier, R.E., Billinge, S.J.L., 2008. Powder Diffraction. Theory and Practice. The Royal Society of Chemistry, Cambridge, UK.
- Dubiński, J., 2013. Sustainable development of mining mineral resources. *J. Sust. Min.* 12 (1), 1–6. <http://dx.doi.org/10.7424/jsm130102>.
- Feng, X. et al., 2002. Occurrence, emissions and deposition of mercury during coal combustion in the province Guizhou, China. *Water Air Soil. Pollut.* 139, 311–324.
- Feret, F.R., 2000. Mining: mineral ores and products. In: Chung, F. H., Smith, D.K. (Eds.), *Industrial Applications of X-ray Diffraction*. Marcel Dekker Inc., New York Basel, pp. 385–413.
- Gibb, W.H. et al., 2000. The fate of coal mercury during combustion. *Fuel Process. Technol.* 65–66, 365–377.
- Głodek, A., Pacyna, J.M., 2009. Mercury emission from coal-fired power plants in Poland. *Atmos. Environ.* 43, 5668–5673.
- Gostomczyk, M.A. et al., 2010. Ograniczenie emisji rtęci z procesów spalania węgla (in Polish: Mitigation of mercury emission from combustion processes). Politechnika Wroclawska, Instytut Techniki Ciepłej i Mechaniki Płynów, Wrocław.
- Hławiczka, S. et al., 2003. Partitioning factor of mercury during coal combustion in low capacity domestic heating units. *Sci. Total Environ.* 312, 261–265.
- Hower, J.C. et al., 2005. Mercury in Eastern Kentucky coals: geologic aspects and possible reduction strategies. *Int. J. Coal Geol.* 62, 223–236.
- Hower, J.C. et al., 2010. Mercury capture by native fly ash carbons in coal-fired power plants. *Prog. Energ. Combust.* 36, 510–529.
- International Energy Outlook, 2013. Energy Information Administration Office of Integrated Analysis U.S. Department of Energy, Washington, 2013. <www.eia.doe.gov/oi/af/ieo/index.html> .
- Jasieńska, S., 1995. Chemia i fizyka węgla (in Polish: Chemistry and physics of coal). Politechnika Wroclawska, Wrocław.
- Kłojzy-Karczmarczyk, B., Mazurek, J., 2010. Rtgę w gruntach w otoczeniu wybranych składowisk odpadów górnictwa węglowego. *Polityka Energetyczna* 13, 245–251.
- Klug, H.P., Alexander, L.E., 1974. *X-ray Diffraction Procedures for Polycrystalline and Amorphous Materials*. John Wiley & Sons, New York.
- Kostova, I. et al., 2013. Influence of surface area properties on mercury capture behaviour of coal fly ashes from some Bulgarian power plants. *Int. J. Coal Geol.* 116–117, 227–235.
- Kutchko, B.G., Kim, A.G., 2006. Fly ash characterization of by SEM–EDS. *Fuel* 85, 2537–2544.
- Market Information Centre <<http://www.cire.pl/rynekenergii/podstawa.php?smid=207>> .
- Michalska, A., 2010. Analysis of mercury content in the environment in the Silesian Voivodeship. *J. Ecol. Health* 4 (82), 165–168.
- Niedźwiecki, E. et al., 2007. Zanieczyszczenie środowiska glebowego metalami ciężkimi przez niekontrolowane wysypiska odpadów. *Ochr. Środ. i Zasobów Naturalnych* 31, 126–130.
- Pacyna, E.G. et al., 2010. Global emission of mercury to the atmosphere from anthropogenic sources in 2005 and projections to 2020. *Atmos. Environ.* 44, 2487–2499.
- Państwowy Instytut Geologiczny, Surowce Mineralne Polski (Polish Geological Institute, Polish Mineral resources) <http://geoportalski.gov.pl/css/surowce/images/2013/tabele/wegle_kamienne_zasoby.pdf> (accessed 4 May 2015).
- Rietveld, H.M., 1969. A profile refinement method for nuclear and magnetic structures. *J. Appl. Crystallogr.* 2, 65–71.
- Rietveld, H.M., 1967. Line profiles of neutron powder-diffraction peaks for structure refinement. *Acta Crystall.* 22, 151–152.
- Rubel, A.M. et al., 2006. Thermal stability of mercury captured by ash. *Fuel* 85, 2509–2515.
- SIROQUANT™ Quantitative XRD Software, 2000. User's Guide and Reference, Ver. 2.5 for Windows.
- Smoliński, A., 2007. Energetyczne wykorzystanie węgla jako źródło emisji rtęci. Porównanie zawartości Hg w wybranych polskich węglach z zawartością tego metalu w węglach na świecie (in Polish: Energy utilization of coal as a source of mercury emission. Comparison of mercury content in selected Polish and world coals), *Ochrona Powietrza i Problemy Odpadów* 2(238), 45–53.
- Smoliński, A., 2008. Gas chromatography as a tool for determining coal chars reactivity in the process of steam gasification. *Acta Chromatogr.* 20 (3), 349–365.
- Sushil, S., Batra, V.S., 2006. Analysis of fly ash heavy metal content and disposal in three thermal power plants in India. *Fuel* 85, 2676–2679.
- Taylor, J. C., Hinczak, I., 2001. Rietveld Made Easy, 145–146.
- Vejahati, F. et al., 2010. Trace elements in coal: associations with coal and minerals and their behavior during coal utilization – a review. *Fuel* 89, 904–911.
- Wang, S.X. et al., 2010. Mercury emission and speciation of coal-fired power plants in China. *Atmos. Chem. Phys.* 10, 1183–1192.
- Yudovich, Ya E., Ketris, M.P., 2005a. Mercury in coal: a review: Part 1. Geochemistry. *Int. J. Coal Geol.* 62, 107–134.
- Yudovich, Ya E., Ketris, M.P., 2005b. Mercury in coal: a review. Part 2. Coal use and environmental problems. *Int. J. Coal Geol.* 62, 135–165.
- Zhang, J. et al., 2007. Preliminary study of trace element emissions and control during coal combustion. *Front. Energy Power Eng. Chin.* 1 (3), 273–279.